

Attribution studies of observed land precipitation changes with nine coupled models

F. Hugo Lambert,^{1,2} Nathan P. Gillett,³ Dáithí A. Stone,² and Chris Huntingford¹

Received 27 May 2005; revised 25 July 2005; accepted 18 August 2005; published 21 September 2005.

[1] Global-land mean observations of 20th century precipitation are compared to modelled values using an optimal regression technique for nine general circulation models. The combined influence of major anthropogenic and natural forcings is detected in five cases. Comparing the accuracy of precipitation and temperature simulation of each model, we find that low temperature simulation accuracy produces low precipitation simulation accuracy, but temperature accuracy does not determine precipitation accuracy in general. Model formulation appears to be more important for accurate precipitation simulation than inclusion of a more complete set of forcings. The implications for possible constraints on land precipitation are discussed. **Citation:** Lambert, F. H., N. P. Gillett, D. A. Stone, and C. Huntingford (2005), Attribution studies of observed land precipitation changes with nine coupled models, *Geophys. Res. Lett.*, 32, L18704, doi:10.1029/2005GL023654.

1. Introduction

[2] Changes in climate have been attributed to external forcings using optimal regression techniques for a variety of climate variables. *Stott et al.* [2000] and *Tett et al.* [2002] attributed changes in large scale near-surface temperature to a combination of natural and anthropogenic factors, *Gillett et al.* [2003] found that changes in sea-surface pressure cannot be explained by natural variability alone and *Barnett et al.* [2001] attributed changes in basin-scale ocean heat content to anthropogenic forcings, for example.

[3] Studies attributing changes in precipitation have lagged behind because observing and modelling precipitation accurately is difficult. A recent study using the HadCM3 model by *Lambert et al.* [2004], however, found an attributable response for global-land precipitation to natural and anthropogenic forcings that appeared to be largely due to volcanic forcing. This was supported by *Gillett et al.* [2004] who detected the influence of volcanic forcing, but not greenhouse gases (GHGs), anthropogenic sulphates or changes in solar irradiance, using the PCM model. Both studies found that the model simulations they used possibly underestimate the observed response to forcing. Further, *Allen and Ingram* [2002] showed that the range of modelled global precipitation responses to global warming varies by a factor of ~ 3 . In this work, we therefore compare observed precipitation to results from

nine state-of-the-art coupled models. We then compare the accuracy of modelled temperature and precipitation and discuss the implications for possible constraints on land precipitation change.

2. Observed and Modelled Data

[4] Observed 20th century precipitation data are compared to simulations from nine General Circulation Models (GCMs). The observations are land-based gauge data taken from the Hulme data set for 1900–98 interpolated onto a 3.75° longitude by 2.5° latitude grid [*Hulme*, 1992; *New et al.*, 2000]. Following *Gillett et al.* [2004], we restrict ourselves to 1944–98, when the largest changes in climate forcings occur.

[5] The modelled data are taken from the IPCC model output archive and were provided by modelling centres for the imminent IPCC Fourth Assessment Report. The simulations are driven with estimates of historical forcings for the 20th century. We consider only models forced with at least the following four factors: changes in GHGs, the direct effect of tropospheric sulphate aerosols, stratospheric volcanic sulphate aerosols and solar irradiance. Some of the models are also driven by changes in the indirect effects of tropospheric sulphates (IS), black carbon aerosol concentration (BC), stratospheric ozone (SO) and land use (LU), see Table 1.

[6] A global land mean time series is calculated for the observations and each GCM. Observed data are masked so that in each year, only gridboxes having data for at least 7 of 12 months are considered. (The series produced is insensitive to this criterion, however.) The mean climatology from 1961–90 is then removed at each spatial point, ensuring that we are only considering anomalies about a base period. The GCM data are masked identically to the observations and anomalies taken with respect to their own climatologies. Each GCM has a minimum of three ensemble members with different initial conditions (Table 1). These are averaged together to improve the signal-to-noise ratio for the detection of forced signals, because we expect model-simulated internal variability to be uncorrelated between ensemble members. Figure 1 shows land mean time series for observed and model data. In the plot, we differentiate between those models forced by IS, and those which are not. There do not appear to be significant differences between the time series, however.

3. Attribution of Changes in Precipitation

[7] We now compare the observed and modelled time series for 1944–98 using the optimal total least squares regression technique described by *Allen and Stott* [2003].

¹CEH Wallingford, Wallingford, UK.

²Department of Physics, University of Oxford, Oxford, UK.

³Climatic Research Unit, University of East Anglia, Norwich, UK.

Table 1. The Size of the Initial Condition Ensemble for Each Model, and Whether or Not It is Forced With IS, BC, SO or LU^a

Model	Runs	IS	BC	SO	LU	Vol	$\beta_{\min}, \hat{\beta}, \beta_{\max}$	Variance Ratio	$\hat{\rho}_{precip}$
GFDL CM2 0	3	No	Yes	Yes	Yes	R	0.79, 1.7, 3.4	0.70	0.70
GFDL CM2 1	3	No	Yes	Yes	Yes	R	-0.99, -0.18, 0.57	0.80	-0.09
GISS Model E H	5	Yes	Yes	Yes	Yes	HS	unbounded	0.33	0.91
GISS Model E R	9	Yes	Yes	Yes	Yes	HS	0.30, 1.3, 2.5	0.35	0.94
MIROC3 2 medres	3	Yes	Yes	Yes	Yes	Yes	0.26, 1.3, 3.6	0.79	0.94
MRI CGCM2 3 2a	5	No	No	No	No	S93	unbounded	0.21	0.87
NCAR CCSM3	8	Yes	Yes	Yes	No	Yes	unbounded	0.29	0.91
NCAR PCM1	4	Yes	No	Yes	No	A	1.3, 3.2, 16.	0.39	0.80
UKMO HadCM3	4	Yes	No	Yes	No	S93	1.0, 1.9, 3.7	0.56	0.48

^aAll nine models are also forced with GHGs, the direct effect of tropospheric sulphate aerosols, volcanic aerosols and changes in solar irradiance. The Vol column shows whether the volcanic forcing comes from C. M. Ammann et al. (Coupled climate simulations of the 20th-century including external forcing, submitted to *Journal of Climate*, 2005), A; Hansen and Sato [2001], HS; Sato et al. [1993], S93; or Ramachandran et al. [2000], R, where known. The β s are the 5–95% range of scaling factors derived from regression. The variance ratio is the average ratio of individual model ensemble member variance to observed variance for 5-year precipitation means from 1944–98. $\hat{\rho}_{precip}$ are the correlations between land and global precipitation for the same averaging periods.

First, 11 5-year means of the observed and modelled time series are taken, because this was the timescale on which Lambert et al. [2004] found forcing to be most dominant. The time series are then projected onto the first 11 Empirical Orthogonal Functions (EOFs) of an identically prepared unforced control run, the minimum number necessary to completely describe the data. Signal-to-noise optimisation is achieved by weighting the resulting components by the inverse of the noise variance of the relevant EOF. The control run used is the same in each case, and consists of data from each model concatenated together, because only a short section of control is available in each case. We do not spatially optimise our data because we are interested in the behavior of and constraints on global land mean precipitation.

[8] Assuming that model response amplitude may be scaled up or down linearly, the regression coefficients, β , that we calculate, inform us whether or not the model is under or overestimating the observed precipitation response to forcing. If the confidence interval that contains β is entirely greater than zero, then we say that the influence of the forcings applied to the model is detected. If the confidence limit includes 1, and the residual observed variance is consistent with an estimate of natural variability derived from the control run, then we say that we have attributed observed changes in precipitation to the forcings applied to the model.

[9] The regression coefficients we obtain for the period 1944–98 are summarised in Table 1. For GFDL0, HadCM3, and PCM we detect the influence of the forcings applied to the model at the 5% level, and find that residual variance is not inconsistent with control variability at the 10% level using the *F*-test, despite these models not being forced with the full range of forcings. We also detect the applied forcings in the case of GISS-ER and MIROC, but find that residual and control variability are marginally inconsistent. The observed residual variance is unrealistically large, suggesting that either the control variance underestimates natural variability, or that significant forced responses are not simulated by the models.

[10] We cannot detect the influence of applied forcings with the other models at the 5% confidence level for 1944–98. GFDL1, and MRI, in particular, fail to capture the observed response (Figure 1). For CCSM3, MRI and GISS-EH the confidence limits that we calculate are

unbounded, indicating that the forced signal in these runs is not significantly different from zero. We can attribute forced precipitation response to forcing in 3 of 9 cases - more than 1 in 20 that we would expect from chance at the 5% level. Still, we conclude that Lambert et al. [2004] and Gillett et al. [2004] were fortunate to employ GCMs that adequately simulate forced changes in precipitation.

[11] We also calculate joint regression coefficients for the nine models using the “error in variables” method of C. Huntingford et al. (Incorporating model uncertainty into attribution of observed temperature change, submitted to *Geophysical Research Letters*, 2005). The method makes an estimate of modelling uncertainty by adding the variance of individual models from the model mean time series to the covariance matrix of control run variability used to form confidence intervals. Giving equal weight to each model, we then form the mean time series across all models and carry out detection as normal. For our nine models, we find 5–95% confidence limits for β that span -27.6 to 6.44, reflecting large differences between models, and the inability of some models to capture observed precipitation changes.

[12] Inspection of Figure 1 suggests that the observations, and those models that successfully mimic them, are chiefly responding to volcanic forcing, which is the cause of the large fluctuations in the lower forcing curve of Figure 1c. This supports the findings of Gillett et al. [2004], who were able to formally attribute observed changes to volcanic forcing, but not to anthropogenic GHGs and sulphates or solar forcings. We cannot follow up their work, because we do not have access to GCM simulations forced with only volcanic forcing. Although only PCM formally underestimates the size of the response (the confidence limits enclosing β are entirely greater than 1), all the models appear to show precipitation changes smaller than those observed. This is confirmed by the ratio of the average variance of individual forced ensemble members to observed variance shown in Table 1, and could be caused by model errors or missing forcings, or measurement errors we have not considered. There is also a small (and statistically insignificant) downward trend in the observations, replicated by MIROC and GISS-ER but not apparent in the other models. We speculate that this may be due to the indirect effects of sulphate aerosols, which are expected to

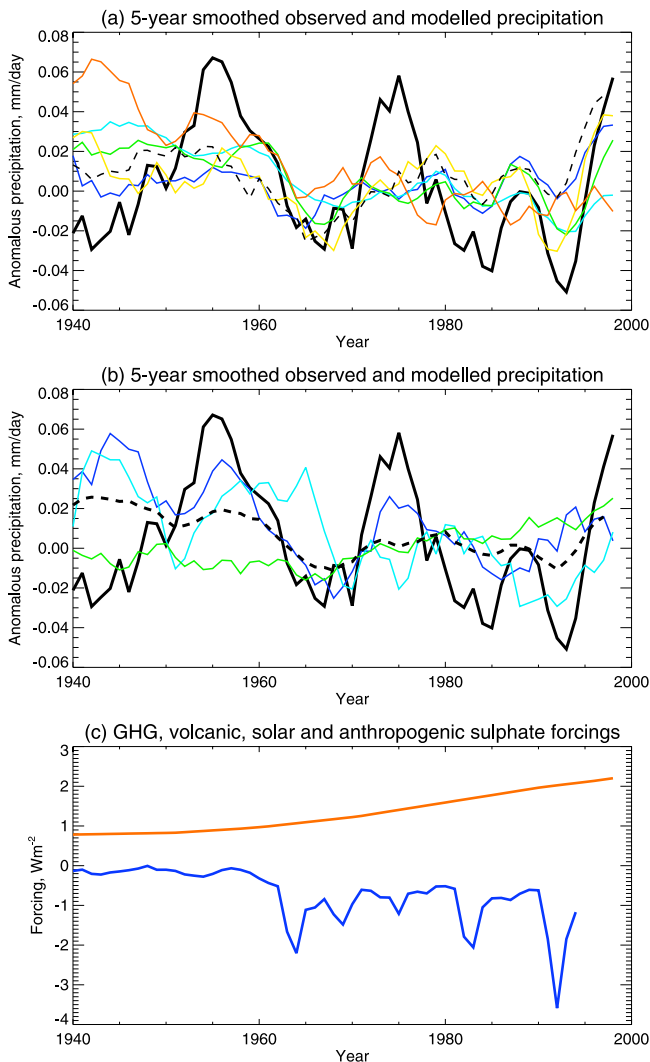


Figure 1. 5-year running averaged global land mean precipitation anomalies with respect to 1961–90 in the better-observed, latter part of the record (1940–98). In Figures 1a and 1b, the solid black line represents observations. (a) Model ensemble mean values prepared identically to observations and forced with IS: CCSM3 (dark blue), GISS-EH (pale blue), GISS-ER (green), HadCM3 (yellow) MIROC (red) and PCM (black dashes). (b) Not forced with IS: GFDL0 (dark blue), GFDL1 (pale blue) and MRI (green). The mean value across all nine model ensembles (and giving equal weight to each model) is plotted as a dashed black line. (c) Unsmoothed global mean annual forcing time series applied to the models. Greenhouse gas forcing is plotted in red. Total anthropogenic sulphate, volcanic and solar forcing is plotted in dark blue.

cause reductions in precipitation through their effects on cloud water.

4. Comparison of Precipitation Simulation to Temperature Simulation

[13] What are key features of the climate system that must be modelled if observed responses to forcing are to be

captured? In the case of temperature, a simple model simulating bulk climate sensitivity and the rate of ocean uptake can reproduce the observed global response [e.g., Sokolov and Stone, 1998]. For precipitation, it has been suggested that a linear model of perturbations to the tropospheric energy budget dependent only on temperature and forcings may be able to predict changes [Allen and Ingram, 2002]. This model can explain why precipitation appears to respond strongly to volcanic forcing, but not to anthropogenic GHGs [see also Mitchell *et al.*, 1987; Yang *et al.*, 2003]. However, it fails to account for large differences in land and global precipitation in some models (see GCM correlations in Table 1), despite very high correlations between land and global temperature (≥ 0.99 for all 9 models) and quite similar changes in forcing [e.g., Ramaswamy *et al.*, 2001]. This was confirmed by Lambert *et al.* [2004], who found the energy budget model successful globally, but less applicable when the data were restricted to land in a GCM simulating only a shallow ocean with no dynamics. From our precipitation correlations it appears that different constraints may be important in different models.

[14] Here we compare the accuracy of global precipitation and temperature simulation in the nine coupled models. Temperature changes are important to both the energy budget argument and soil moisture levels, which were cited as a possible alternative constraint on land precipitation changes by Koster *et al.* [2004]. Figure 2 shows the root mean squared difference between modelled and observed global mean temperature and precipitation for individual ensemble members. (The observed temperature data are taken from CRUTEMP2(v) [Jones and Moberg, 2003].) The bottom right corner of the figure is devoid of points, indicating that a poor simulation of temperature guarantees a poor simulation of precipitation. A good simulation of temperature, however, does not guarantee a good simulation of precipitation. Examining individual models, we see that temperature and precipitation accuracy in CCSM3 may be linearly related, GISS-ER shows large variations in precipitation accuracy unrelated to temperature and MRI shows large variations in temperature accuracy unrelated to precipitation. It is more difficult to draw conclusions for the models with fewer ensemble members, but we note that HadCM3 and GISS-EH consistently provide accurate simulations and PCM shows little variation in accuracy, consistent with the small natural precipitation variability shown by the model. The differences between individual ensemble members are comparable to the differences between models. As in Section 3, we conclude that the models driven with all eight forcings do not provide significantly better simulations. Differences in model formulation appear to be more important.

5. Conclusion

[15] We detect the influence of applied forcings on global-land mean precipitation in five of nine coupled GCMs for 1944–98. While the forcings we consider are sufficient to explain the bulk of observed precipitation changes during this period using five models, we see that model formulation is important for successful detection. This is confirmed where we incorporate modelling

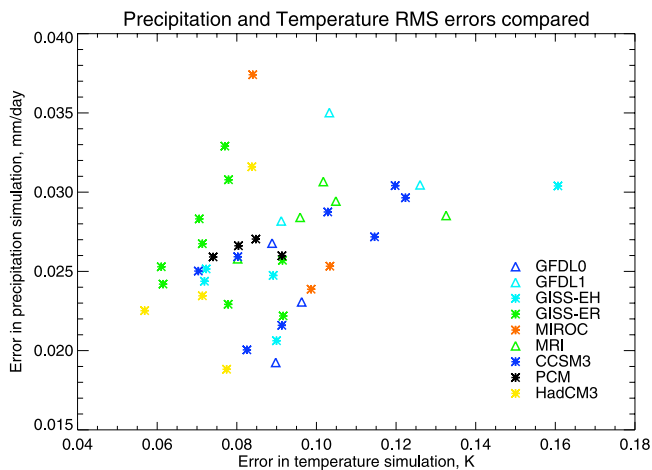


Figure 2. Accuracy of precipitation and temperature simulation compared. For each model ensemble member, the root mean squared difference with observations is calculated for the 11 5-year means between 1944 and 1998. The ensemble members are plotted with the same colour coding as in Figure 1 with models from Figure 1a represented as stars and models from Figure 1b as triangles.

uncertainty into a single multi-model detection experiment: we do not detect the applied forcings and find a large range for the possible signal amplitude. This differs from the surface temperature case where detection results are fairly consistent for the same models (D. A. Stone et al., A multi-model update on the detection and attribution of global surface warming, submitted to *Journal of Climate*, 2005). Although realism of temperature response is important to two precipitation constraints we discuss, we find that it does not fully determine realism of precipitation response. Given the wide range of responses of the nine models, if a simple constraint on land precipitation changes does exist, it does not appear to be a ubiquitous feature of GCMs. More study is needed if we are to find how observed land precipitation is controlled.

[16] **Acknowledgments.** We thank Mike Hulme at the Tyndall Centre for Climate Change Research at the University of East Anglia (UEA) for the observed precipitation data set. We acknowledge the international modeling groups for providing their data for analysis, the Program for Climate Model Diagnosis and Intercomparison (PCMDI) for collecting and archiving the model data, the JSC/CLIVAR Working Group on Coupled Modelling (WGCM) and their Coupled Model Intercomparison Project (CMIP) and Climate Simulation Panel for organizing the model data analysis activity, and the IPCC WG1 TSU for technical support. The IPCC Data Archive at Lawrence Livermore National Laboratory is supported by the Office of Science, U.S. Department of Energy. We also thank Myles Allen, who originally developed the optimal detection code used here, and

Peter Stott for a useful discussion. We thank two referees for thorough reviews. FHL acknowledges financial support from CEH.

References

- Allen, M. R., and W. J. Ingram (2002), Constraints on the future changes in climate and the hydrological cycle, *Nature*, *419*, 224–232.
- Allen, M. R., and P. A. Stott (2003), Estimating signal amplitudes in optimal fingerprinting, part I: Theory, *Clim. Dyn.*, *21*, 477–491.
- Barnett, T. P., D. W. Pierce, and R. Schnur (2001), Detection of anthropogenic climate change in the world's oceans, *Science*, *292*, 270–274.
- Gillett, N. P., F. W. Zwiers, A. J. Weaver, and P. A. Stott (2003), Detection of human influence on sea level pressure, *Nature*, *422*, 292–294.
- Gillett, N. P., A. J. Weaver, F. W. Zwiers, and M. F. Wehner (2004), Detection of volcanic influence on global precipitation, *Geophys. Res. Lett.*, *31*, L12217, doi:10.1029/2004GL020044.
- Hansen, J. E., and M. Sato (2001), Trends of measured climate forcing agents, *Proc. Natl. Acad. Sci.*, *98*, 14,778–14,783, doi:10.1073/pnas.261553698.
- Hulme, M. (1992), A 1951–80 global land precipitation climatology for the evaluation of general circulation models, *Clim. Dyn.*, *7*, 57–72.
- Jones, P. D., and A. Moberg (2003), Hemispheric and large-scale air temperature variations: An extensive revision and an update to 2001, *J. Clim.*, *16*, 206–223.
- Koster, R. D., et al. (2004), Regions of strong coupling between soil moisture and precipitation, *Science*, *305*, 1138–1140.
- Lambert, F. H., P. A. Stott, M. R. Allen, and M. A. Palmer (2004), Detection and attribution of changes in 20th century land precipitation, *Geophys. Res. Lett.*, *31*, L10203, doi:10.1029/2004GL019545.
- Mitchell, J. F. B., C. A. Wilson, and W. M. Cunningham (1987), On CO₂ climate sensitivity and model dependence of results, *Q. J. R. Meteorol. Soc.*, *113*, 293–322.
- New, M., M. Hulme, and P. Jones (2000), Representing twentieth-century space-time climate variability. Part II: Development of 1901–96 monthly grids of terrestrial surface climate, *J. Clim.*, *13*, 2217–2238.
- Ramachandran, S., V. Ramaswamy, G. L. Stenchikov, and A. Robock (2000), Radiative impacts of the Mt. Pinatubo volcanic eruption: Lower stratospheric response, *J. Geophys. Res.*, *105*, 409–424.
- Ramaswamy, V., J. Haigh, D. Hauglustaine, J. Haywood, G. Myhre, T. Nakajima, G. Y. Shi, and S. Solomon (2001), Radiative forcing of climate change, in *Climate Change 2001: The Scientific Basis: Contribution of Working Group I to the Third Assessment Report of the Intergovernmental Panel on Climate Change*, edited by J. T. Houghton et al., pp. 349–416, Cambridge Univ. Press, New York.
- Sato, M., J. E. Hansen, M. P. McCormick, and J. B. Pollack (1993), Stratospheric aerosol optical depth, 1850–1990, *J. Geophys. Res.*, *98*, 22,987–22,994.
- Sokolov, A. P., and P. H. Stone (1998), A flexible climate model for use in integrated assessments, *Clim. Dyn.*, *14*, 291–303.
- Stott, P. A., S. F. B. Tett, G. S. Jones, M. R. Allen, J. F. B. Mitchell, and G. J. Jenkins (2000), External control of 20th century temperature by natural and anthropogenic forcings, *Science*, *290*, 2133–2137.
- Tett, S. F. B., et al. (2002), Estimation of natural and anthropogenic contributions to twentieth century temperature change, *J. Geophys. Res.*, *107*(D16), 4306, doi:10.1029/2000JD000028.
- Yang, F., A. Kumar, M. E. Schlesinger, and W. Wang (2003), Intensity of hydrological cycles in warmer climates, *J. Clim.*, *16*, 2419–2423.

N. P. Gillett, Climatic Research Unit, University of East Anglia, Norwich NR4 7TJ, UK.

C. Huntingford, CEH Wallingford, Maclean Building, Crowmarsh Gifford, Wallingford OX10 8BB, UK.

F. H. Lambert and D. A. Stone, Atmospheric, Oceanic and Planetary Physics, Clarendon Laboratory, Parks Road, Oxford OX1 3PU, UK. (hlambert@atm.ox.ac.uk)